Earth's rotation and Earth-Moon distance in the Devonian derived from multiple geological records

Christian Zeeden, Jacques Laskar, David de Vleeschouwer, Damien Pas, Anne-Christine da Silva

Version of Record: https://www.sciencedirect.com/science/article/pii/S0012821X23003618
Manuscript_6a97aefce88d2342f3feda50610454ef

Earth's rotation and Earth-Moon distance in the Devonian derived from multiple geological records

Christian Zeeden[1,2], Jacques Laskar[1], David De Vleeschouwer[4], Damien Pas[5] Anne-Christine Da Silva[3],

[1]) IMCCE, Observatoire de Paris, PSL Research University, CNRS, Sorbonne Universités, 75014 Paris, France

[2]) LIAG - Leibniz Institute for Applied Geophysics, Stilleweg 2, 30655 Hannover, Germany

[3]) Pétrologie sédimentaire, B20, Allée du Six Août, 12, Quartier Agora, Liège University, Sart Tilman, 4000 Liège, Belgium

[4]) Institute of Geology and Paleontology, Westfälische Wilhelms-Universität (WWU) Münster, Corrensstr 24, 48149 Münster, Germany

[5]) Institute of Earth Sciences (ISTE), University of Lausanne, CH-1015 Lausanne, Switzerland

Abstract

Astronomical insolation forcing plays an important role in pacing Earth's climate history, including paleoclimate dynamics, and its imprint can be seen in various geoarchives. Its signature is often evident through typical rhythmic patterns in sediments. The detailed study of those patterns led to a better understanding of orbital climate forcing, while also providing more precise constraints on the geological time scale. Due to the tidal evolution in the Earth-Moon system, the precession and obliquity periods get shorter when going back in time while the main eccentricity 405 kyr period remains stable. While several astrophysical models describe the evolution of the length of precession- and obliquity cycles, few reliable and quantitative geological information from tidalites and astrochronology are available.

To better constrain these key astronomical parameters in the distant past, we calculate precession and obliquity properties for the Devonian (~420-360 million years before present) as reconstructed from a suite of geological datasets. Our results show the period of precession to be 19.4-16.1 kyr, and the dominant p+s3 obliquity period to be 29.50±0.46 long. These findings are compared with and support the presence of oceanic tidal resonances at 300 and 540 Ma, as shown in the recent AstroGeo22 model of the Earth-Moon evolution of (Farhat et al, 2022).

1. Introduction

Since the work of George Darwin (1879), it is known that due to the tidal interaction between the Earth and the Moon, the rotation of the Earth slows down and the Moon moves away from Earth. This phenomenon was first measured through ancient eclipses, and since 1969 with laser ranging on reflectors deposited on the Moon by Apollo astronauts. The continuing distance escape rate is recently 3.83 cm/year (Williams and Boggs, 2016). The age of the Moon is now also well determined at 4.425 Ga, also thanks to the Apollo missions (e.g., Maurice et al., 2020). More than fifty years ago it was realised that with the present tidal recession rate of the Moon, Darwin's tidal model leads to a collision of the Moon with the Earth at about 1.5 Ga (Gerstenkorn, 1967), incompatible with the age of the Moon. Since then, many works have been devoted to resolve this paradox. Until recently, no physical model accounted for both the age of the Moon and the present Lunar recession rate (Daher et al., 2021; Green et al., 2017; Tyler, 2021; Webb, 1980).

To overcome this issue, studies have often relied on empirical models fitted to the available geological evidences (Berger and Loutre, 1994; Walker and Zahnle, 1986; Waltham, 2015). With the release of the solution of Farhat et al. (2022) for the evolution of the Earth-Moon system, this situation has changed. Their model is a physical model, following (Webb, 1980), but is improved through taking the continental evolution over the most recent Ga into account, and including the transition to a global ocean in the ancient eons. The Farhat et al. (2022) model has only two parameters, representing the average depth of the ocean and a dissipation factor in the bottom of the ocean. With a proper adjustment of these two parameters, their model (AstroGeo22)[1], gives a match to the present tidal recession and the age of the Moon (Farhat et al., 2022), and also to most cyclostratigraphic data. AstroGeo22 has the potential to become the standard of reference for the Earth-Moon evolution. Yet, it is crucial to continue acquiring reliable geological data in order to confront AstroGeo22, and all models, with geological evidence - especially in the most critical parts that correspond to oceanic tidal resonances (Farhat et al., 2022). Recently, four additional points have been provided to be compared to astronomical solutions, at 259, 455, 655, and 2465 Ma (Zhou et al., 2022), using the TimeOptMCMC method of Meyers and Malinverno (2018). In the present work, we use a different cyclostratigraphic method to derive an additional precession point at 400 Ma, a critical location for the validation of the AstroGeo22 model and an additional data point for comparison with other models.

Cyclostratigraphy is an established part of integrated stratigraphy, utilizing the quasi-periodic variations of precession, obliquity and eccentricity and their amplitudes as geochronometer (e.g. Hilgen et al., 2015; Hinnov and Hilgen, 2012). This approach is based on the identification of

[1] https://www.astrogeo.eu/

Milankovitch cycles in the sedimentary record. Their principal components include long and short eccentricity (405/~100 kyr), and their amplitude modulations (2.4 Myr, very long eccentricity); axal tilt or obliquity (with a present period of about 41 kyr) and its amplitude modulation dominated by a 1.2 Myr cycle; as well as climatic precession (recently ~20 kyr, modulated by eccentricity). Orbital and rotational solutions provide insolation properties for Earth's past and future. Geoarchives can be correlated to the solutions as 'astronomical tuning', allowing their application as a geochronometer. Also, the parametrization of orbital solutions can be tested through comparison with geological data (Lourens et al., 2001; Zeeden et al., 2013, 2014). Orbital solutions can be computed back back in time (and also for the future) up to about 50 Ma (Laskar et al., 2011a, 2011b). Nevertheless, the 405 kyr eccentricity component is especially stable through Earth history and can be used as a reference chronometer for the determination of the past precession frequency of the Earth through the sedimentary archive (Laskar et al., 2004).

For the reconstruction of astronomical properties, one may investigate the best suitable datasets which are available. This is commonly done in Neogene reconstructions (Lourens et al., 2001; Meyers and Malinverno, 2018; Zeeden et al., 2014, 2013), where relatively noise-free high-resolution data featuring a visually clear expression of precession, obliquity and precession are available. Also for the Paleoproterozoic, clearly expressed Milankovitch cycles have been reported (Lantink et al., 2022). However, generally, deep marine records are sparse for times older than the recent ocean floor (Middle Jurassic) (Ruddiman, 2001). When going back in time, such datasets with clear and visually identifiable expression of Milankovitch cycles in outcrops become sparse or unavailable, and the need to use also noisier datasets becomes apparent for times where no other datasets are available. For this reason, we developed a new approach that enables the integration of relatively noisy geological proxy records with a demonstrated orbital imprint for the calculation of the precession and obliquity cycle periods, and the underlying precession constant k. We name this approach 'CTest', short for consistency test between geological observations and astronomical constraints. Conceptually, this approach requires confidence that neither noise nor distortions of frequency spectra through sedimentary processes (e.g., Fischer et al., 1991) change the frequency ratio of astronomical climate forcing. In our approach, we test the orbital imprint of multiple individual datasets for consistency, and in this way we provide more confidence in unideal datasets, and aim to reduce uncertainty of k. While in theory also assessment of the g2 to g5 and s3 components is possible, the here analysed datasets did not allow confined statements on their frequency. The g2-g5 terms represent precession of the perihelions for planets, and the s3 term is related to precession of the orbital plane of Earth. We determine the frequency of dominant precession and obliquity components, and also the underlying precession constant p, with their respective uncertainty for the Devonian ca. 420-360

million years before present. Through analyses of eight (sub)datasets of similar age (Figs. 1, 2) we can increase confidence through consistency of these datasets. Further, we increase precision through calculating a combined probability.

2. Datasets

In this study, we use four published magnetic susceptibility records and divide these into eight sub-datasets covering most of the Devonian (Da Silva et al., 2016, 2013; De Vleeschouwer et al., 2015; Pas et al., 2018; Tab. 1; Figs 1, 2) and the interpretations of these in terms of Milankovitch insolation forcing in the Devonian. The Lower Devonian records from the Prague Basin sedimentologically represents the carbonate distal offshore facies, and are composed of hemipelagic clayey limestones intercalated by submarine landslide deposits (synthesis in Da Silva et al., 2016, and references therein). The Middle Devonian records from the Rhenish Basin (Baileux and La Thure) are mainly composed of shallow-water carbonates deposited either within the ramp, the fore-reef or the rimmed-shelf (Da Silva et al., 2013; Mabille and Boulvain, 2008; Pas et al., 2017). The Upper Devonian record form the Sullivan core (Illinois Basin, USA) is mainly composed of shales, siltstone and calcareous shale deposited in deep-shelf environments (Pas et al., 2018, and references therein). All these records were tested for diagenetic alteration, pointing to a good preservation of the primary information versus secondary imprint (Da Silva et al., 2013, 2016, 2019; Pas et al., 2017).

While all used datasets show a clear orbital imprint, and quasi-cyclic behavior at different frequencies related to orbital climate forcing, it is possible that not all individual cycles are present in the datasets, as intervals of low deposition/preservation may occur. Datasets and derived sedimentation rates are consistent with biostratigraphical constraints. We regard our statistical assessment robust for assessing the periodograms of the datasets, and do not see an issue with utilizing the shallow marine possibly incomplete datasets. In this relatively shallow marine setting, not all outcrops/datasets visually show obvious cyclicity. In such cases, one would not put heavy weight on individual datasets. However, datasets are from different localities (Fig.1), making common systematic error unlikely. . Although datasets are not from the exact same time interval, but from different stages within the Devonian, we treat these as time-equivalent. This is to allow uncertainty propagation to establish a reconstruction of Milankovitch forcing for the whole Devonian. This is motivated by the considerable uncertainty of k reconstructions derived from individual datasets (Tab. 1, Fig., 4).

The aforementioned studies interpret frequency ranges as eccentricity, obliquity and most studies also interpret climatic precession (Fig. 2). Here, we interpret the 405 kyr eccentricity cycle as identified

in the studied Devonian records as g2-g5, the interpreted short eccentricity frequency range related to the ~95-130 kyr as including the astronomical components g3-g2, g4-g2 (lower frequencies) and g4-g5, g3-g5 (higher frequencies). In cases where double peaks were found in the frequency range related to ~100 kyr eccentricity, interpretations regarding the lower vs. higher frequency eccentricity components in this interval (g3-g2, g4-g2/ g4-g5, g3-g5) were made in addition. The obliquity related peaks in the Devonian records are here interpreted as k+s3 component, because it is the dominant obliquity component (Laskar et al., 2004). The frequency ranges of climatic precession frequency were used from original studies, but in some cases more specific interpretations were made. These concern specifically which peaks in periodograms correspond to the low frequency component k+g5 (recently 23.69 kyr duration), the medium frequency component k+g2 (recently 22.39 kyr duration) and short frequency components (combined k+g4, k+g5; recently 18.96 and 19.10 kyr duration) were made. Details of the Milankovitch interpretations of the Devonian dataset's periodograms are listed in Supplements.

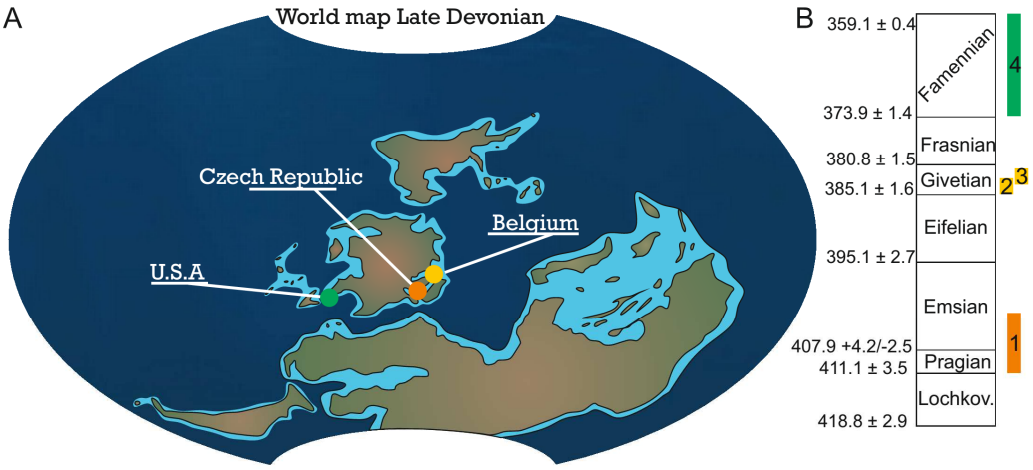

Figure 1: A) Paleogeographic locations of magnetic susceptibility data used in this study (modified after De Vleeschouwer et al., 2017), and their respective intervals within the Devonian time scale (B, after De Vleeschouwer and Parnell, 2014). 1: dataset from Pod Barrandovem in the Czech Republic (Da Silva et al., 2016), 2 and 3 data from Baileux (Da Silva et al., 2013) and La Thure (De Vleeschouwer et al., 2015) in Belgium respectively, and 4 data from the Sullivan core in the US (Pas et al., 2018).

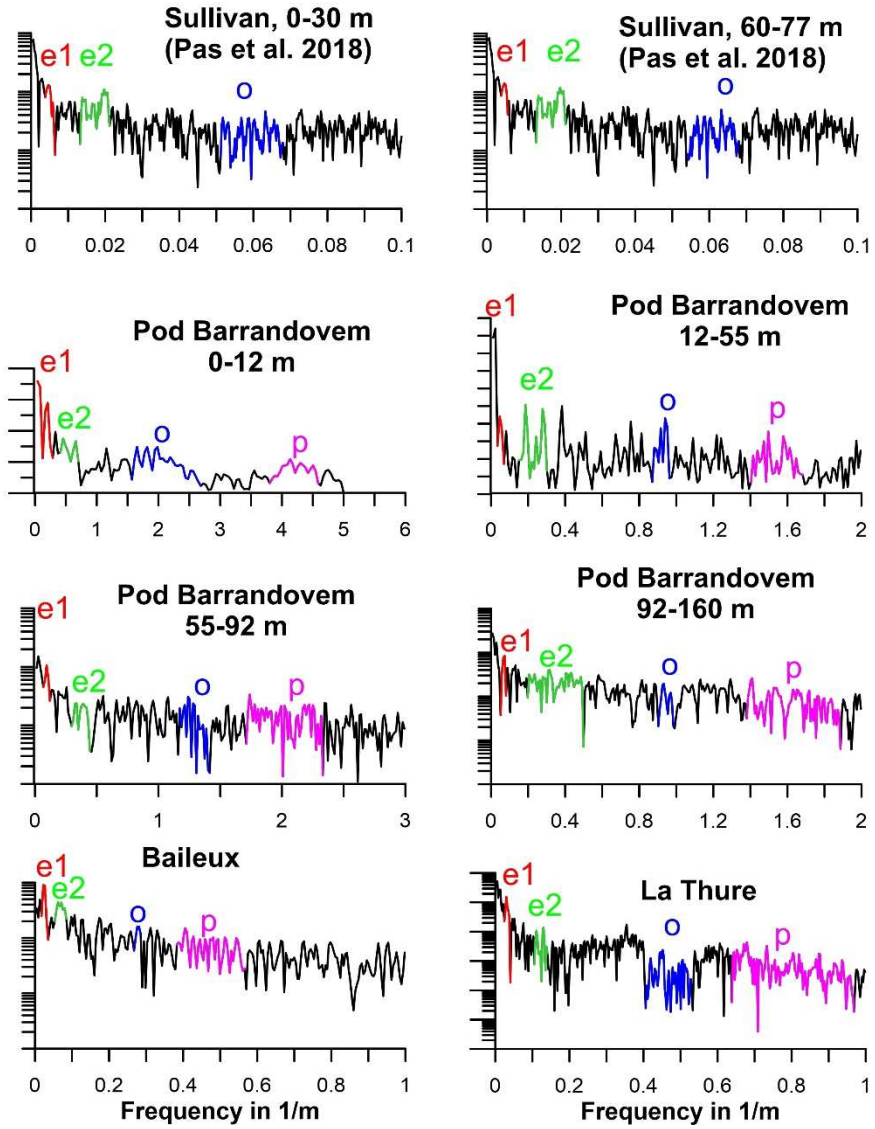

Figure 2: Periodograms showing the frequency components of Devonian magnetic susceptibility datasets (abscissa) versus their power (ordinate) and their cyclostratigraphic interpretation based on original studies (Da Silva et al., 2016, 2013; De Vleeschouwer et al., 2015; Pas et al., 2018). The interpretation regarding the 405 kyr (e1, red) and the ~ 100 kyr eccentricity (94-131 kyr; e2, green) components, obliquity (o, blue) and precession components (p, magenta) is included as colour scheme. Note that the precession components were not interpreted in the Sullivan core (Pas et al., 2018).

3. Methods

We developed a method to extract orbital properties from geological datasets in the depth domain using five steps. Generally, the CTest approach relies on the identification of frequency ranges of eccentricity, obliquity and precession. Sedimentation rate is assessed based on the interpretation of

eccentricity peaks in periodograms. The CTest method samples orbital components: p, g- and s-frequencies from Laskar et al., (2004), within specified bounds as outlined on the next paragraph. CTest then tests if these orbital frequencies are consistent with frequency components from the geological data and the interpretation of periodograms (Fig. 2). Geological data are interpreted in the depth domain (and not on a tuned time scale) to avoid imposing orbital signals upon records through frequency modulation (Huybers and Aharonson, 2010; Zeeden et al., 2019).

Initially, we (a) assess sedimentation rate based on eccentricity components only. In practice, this is done through calculating maximum and minimum sedimentation rates consistent with the interpretation of 405- and ~100 kyr eccentricity-related components. This sedimentation rate range is resampled as an uniform distribution between minimum- and maximum possible values. Next, we (b) resample the deposition time (age of the deposit in Ma) from a uniform distribution between conservative estimates for minimum and maximum age. Following, we (c) resample the precession constant (Laskar et al., 2004) with high uncertainty from a uniform distribution, for the Devonian we used very large boundaries of 10,000 to 26,000 years. For the data from the Walvis Ridge (~55 Ma) and Xiamaling formation (~1400 Ma) rages of k are set to 5,000 – 26,000 years and 18,000 – 30,000 years, respectively. These were set in a range which is clearly wider than a realistic range for k, to avoid imposing result through choice of the initial k to be tested. In the next step, we (d) sample g2-g5 and s3 frequencies. The uncertainty is sampled as normal distribution with standard deviation as a linear extrapolation of the uncertainty given in Laskar et al., (2011a) (their Tab. 6). Next, we (e) test the consistency of the sampled astronomical parameters and sedimentation rate with observed cycles and their interpreted frequency range. If consistent, parameters are saved, otherwise discarded. This procedure was repeated until 1000 consistent results were generated for every data(sub)set. A combined Devonian probability is calculated as multiplication of the probability density distributions from all datasets. The method thus provides zero probability for values inconsistent with any given dataset. An R function, R scripts and an extended documentation for reproducing all experiments are available as supplementary information.

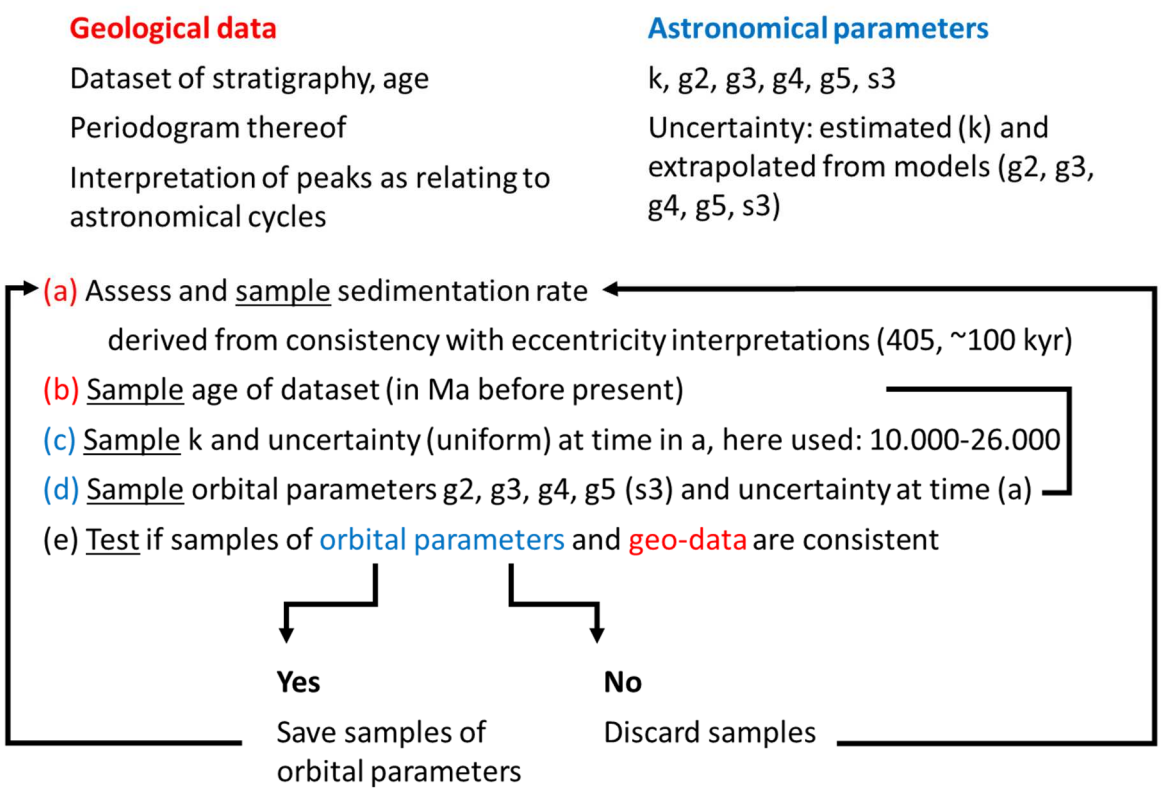

Figure 3: Schematic summary of the CTest approach deriving orbital components k, g2, g3, g4, g5, and s3, where s3 is only derived if an obliquity component is analysed. Note that the uncertainty for k is sampled as a uniform distribution, whereas uncertainty for k, g2, g3, g4, g5, and s3 is taken and extrapolated from (Laskar et al., 2011a). Red text highlights steps using geological data, blue text represents steps done using astronomical theoretical parameters.

4. Results: Devonian Milankovitch cycle durations

To independently test our approach, we applied the CTest method to the Eocene deep sea a* record of the Walvis Ridge (Zachos, 2004), and the ca. 1.4 Ga Xiamaling Formation (Zhang et al., 2015). These datasets were previously analysed in Meyers and Malinverno (2018) using a Bayesian optimisation approach. Results obtained with our CTest method are consistent with the results obtained in Meyers and Malinverno (2018), but CTest retains higher uncertainty in sedimentation rate (vs. optimisation; see Tab. 1).

Testing of a clear precession amplitude relationship with eccentricity led to significant (at >80% confidence using the (Baddouh et al., 2016; Ebisuzaki, 1997) approach for testing significance as implemented in the 'surrogateCor' {astrochron} function (Meyers, 2014)) results for most Devonian datasets showing precession in the depth domain. The lowermost part of the Pod Barrandovem (0-12 m) dataset failed such a test. Therefore, the CTest results of this dataset are reported, but not considered in a combined Devonian estimate (Fig. 4).

The CTest results from all individually Devonian datasets analysed her give consistent durations for precession, obliquity and the underlying precession constant. Figure 4 shows the probability density distributions from all investigated datasets; Tab. 1 summarizes the results. When combining the results from multiple datasets through consideration of shared probability, uncertainty can be reduced, as demonstrated in this study through the more confined combined uncertainty of k (Fig. 4, Tab.1). Here we calculate the obliquity length in the Devonian (~400 Ma) to be 28.79±0.49 kyr (recent: 40.98 kyr). The long (p+g5), intermediate (p+g2) and short precession components (here: combined p+g3, p+g4) are estimated to have been 19.00±0.45 kyr (recent: 23.67 kyr), 18.16±0.41 kyr (recent: 22.36 kyr), and 15.91±0.38 (recent: 19.10, 18.94) kyr in duration, respectively. The precession constant is determined at 20.3±0.25 kyr (recently 25.68 kyr). If considering the mean of all k reconstructions (also inconsistent with other datasets), k is calculated to 21.01 ±1.19 kyr.

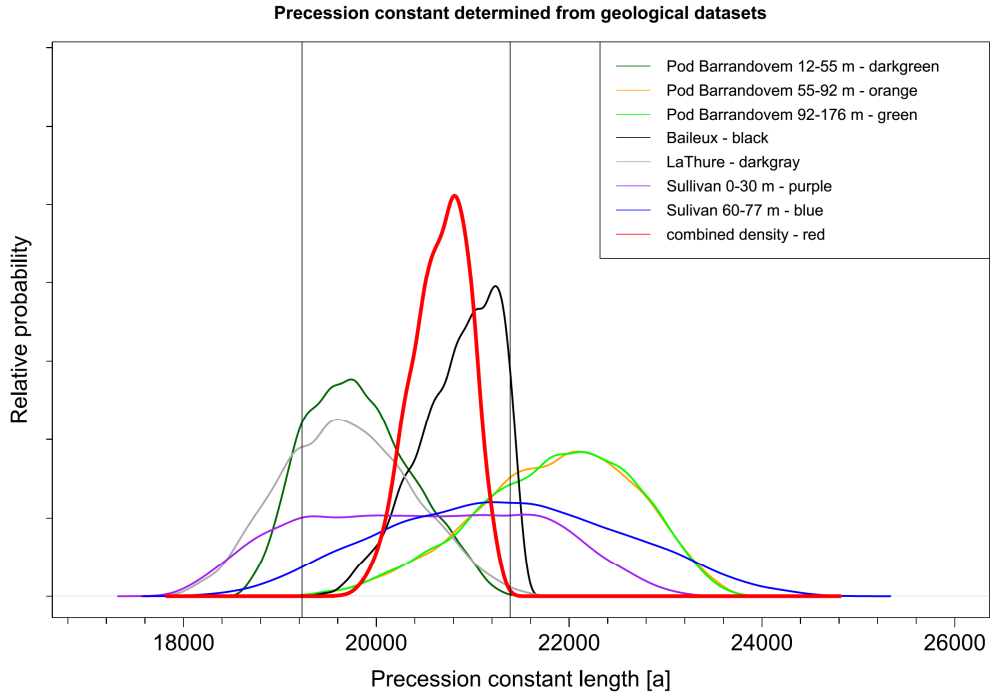

Fig. 4: Reconstructed precession constant (p) from seven Devonian datasets where relative probability (ordinate) is plotted versus the duration of the precession constant in years (abscissa). The bottom part of the Pod Barrandovem dataset (0-12 m) was not considered because it does not show statistically significant precession- or short eccentric amplitude variations. The combined probability is plotted in red, vertical lines indicate the boundaries of shared values for the precession length of all datasets. The resulting precession constant k is calculated to 20.70±0.22 kyr using the abovementioned uncertainty assessment.

Table 1: Reconstructed precession constant (p), precession- and obliquity periods for eight Devonian (sub)datasets (first 8 rows), a Devonian synthesis, and several reference data. Note that data from the 0-12m interval from Pod Barrandovem are not included in the Devonian synthesis, and that data from the Sullivan core (Pas et al., 2018) do not reliably record precession but allow reconstruction of obliquity. Uncertainty is given as 1-sigma here. Data from models and literature are marked bold, the remaining data were derived using the CTest method.

Data	Age in Ma	p [kyr]	p+g5 [kyr]	p+g2 [kyr]	p+g4 [kyr]	p+g3 [kyr]	p+s3 [kyr]
Pod Barrandovem, 0-12m	~408-411	18.53±0.67	17.47±0.60	16.74±0.55	14.87±0.46	14.85±0.45	25.39±1.27
Pod Barrandovem, 12-55m	~407-409	19.82±0.54	18.60±0.48	17.79±0.43	15.63±0.37	15.64±0.39	27.85±1.07
Pod Barrandovem, 55-92m	~405-407	21.85±0.83	20.39±0.72	19.41±0.65	16.77±0.53	16.83±0.53	32.07±1.77
Pod Barrandovem, 92-160m	~403-406	21.85±0.83	20.39±0.72	19.41±0.65	16.77±0.53	16.83±0.54	32.06±1.77
Baileux	~386-390	20.85±0.42	19.52±0.37	18.62±0.33	16.16±0.27	16.19±0.27	29.94±0.86
La Thure	~370-400	19.69±0.68	18.50±0.60	17.69±0.55	15.50±0.47	15.51±0.46	27.62±1.33
Sullivan core, 0-30 m	~365-373	21.54±1.48	-	-	-	-	31.48±3.16
Sullivan core, 60m-top	~359-368	21.33±1.21	-	-	-	-	30.98±2.56
combined Devonian	~359-411	20.70±0.22	19.35±0.20	18.47±0.18	16.13±0.23	16.18±0.16	29.50±0.46
La2004 model, Devonian	385	20.29	19.02	18.17	15.95	15.85	27.78
Farhat et al., 2022 model	385	21.2	19.82	18.89	16.39	16.51	30.64
Berger & Loutre 1994	385	21.98	*20.5*	*19.51*	16.86	16.98	32.31
Eocene WR	~55	25.88±1.01	23.85±0.86	22.52±0.76	19.06±0.56	19.20±0.56	-

Xiamaling formation	~1400	15.76±1.32	14.98±1.20	14.44±1.11	12.95±0.94	12.99±0.94	-
La2004 model, used as test	0	25.37	23.42	22.14	18.79	18.92	40.25
La2004 model, recent	0	25.68	23.68	22.37	18.95	19.10	40.98

240

241

242

243 **5. Discussion**

244 The CTest approach combines cyclostratigraphic data, statistics and astronomical theory to improve
245 our understanding of Earth's rotation history. This method is especially powerful when information
246 from several datasets is combined. Several previous studies have provided reconstructions (e.g., Bond
247 et al., 1991; Fang et al., 2016; Hinnov, 2013; Lantink et al., 2022; Lourens et al., 2001; Meyers and
248 Malinverno, 2018; Williams, 1991; Wu et al., 2018, 2013; Zeeden et al., 2014; Zhou et al., 2022) (e.g.
249 Bond et al., 1991; Fang et al., 2016; Hinnov, 2013; Williams, 1991; Wu et al., 2018, 2013) of the
250 precession constant from geological archives influenced by Milankovitch forcing, and also using the
251 interpretation of tidal rhythmites (tidalites). It should be noted that the analysis of tidalites and
252 bioarchives is undoubtedly valuable. Yet (as for astrochronology) it is depending on the correct
253 interpretation of tidal cycles as such, leaving space for re-interpretation and bias (de Winter et al.,
254 2020; Heubeck et al., 2016; Meyers and Malinverno, 2018; Williams, 1989). The completeness of the
255 deposits is difficult to prove, and relatively little experience exists with such datasets. Further, usually
256 only one or few tidal cycles are preserved consecutively, making statistical analyses challenging. .

257 The CTest approach does not the use of datasets with a clear, and possibly even visually present,
258 astronomical forcing. Instead, it requires datasets showing spectral properties related to eccentricity,
259 obliquity and possibly precession. CTest can use either the expression of obliquity, precession, or both,
260 to determine p. One may argue that unideal datasets are likely noisy in both proxy data and
261 sedimentation rate, as can be seen in evolutive harmonic analyses of datasets in (Da Silva et al., 2016;
262 Pas et al., 2018). Sedimentary noise has the potential to change (frequency) properties of insolation,
263 and can be expected in shallow marine strata due to changing base level, complex sedimentation
264 processes, and possible reworking by wave action in some environments. Therefore, we interpreted
265 the frequency range especially of precession rather wide. In our opinion, noise makes the detailed
266 interpretation of individual datasets especially from the shallow marine realm challenging, but
267 consistent findings in multiple datasets provides confidence allowing interpretations. The clearer and
268 certain the orbital origin of quasi-regular cycles in a dataset, the more robust results will be. In

addition, the more independent constraints on sedimentation rate and on completeness exist, the better. These may come from detailed sedimentological analyses, and dating from e.g., magneto- or bio-stratigraphy. One may argue that deriving information from one such dataset may lead to misinterpretation. Yet, in absence of more suitable datasets with clearly visible cycles and cycle amplitudes of precession/eccentricity and/or short eccentricity/long eccentricity origin, and the analyses of multiple datasets, we regard our approach useful. At the same time we advocate for preferentially utilizing highest quality datasets, and analysing these using both visual (Lantink et al., 2022) and quantitative methods (as CTest and timeOptMCMC; Meyers and Malinverno, 2018). Generally, we argue that a dataset should have such an amplitude relationship to be used for reconstructing astronomical properties, because these are strong arguments for a real imprint of Milankovitch cycles (Meyers, 2015; Meyers and Malinverno, 2018; Shackleton et al., 1995; Zeeden et al., 2019, 2015). Using amplitude relationships as argument for a forcing by Milankovizch cycles also avoids challenges related to frequency spectra and their significance tests.

To evaluate CTest, we have reconstructed the results provided by Meyers and Malinverno, (2018; see Tab. 1) using CTest. CTest results in a higher degree of uncertainty, due to the inclusion of higher uncertainty in the sedimentation rate and the retention of wider spread of sedimentation rates in the results, e.g., for the Xiamaling Formation a range of 0.25 to 0.44 cm/kyr (vs. ~0.33 to ~0.38 from the TimeOptMCMC approach). Although within uncertainty, our approach leads to longer climatic precession cycles in the Protoerozoic than Meyers and Malinverno, (2018). This is due to the strict interpretation of the precession components in our case (Supplementary Fig. 2), and vanishes if the same upper/lower limits for all precession components are used.

While the TimeOptMCMC uses a combination of spectral properties and amplitude relationships of precession and eccentricity, our method also utilizes and provides results for the obliquity component. Obliquity is longer than precession (obliquity is recently~41 kyr, while precession has several components around 20 kyr; Tab.1) which may be regarded as potentially less impacted by high-frequency noise and/or too low sedimentation rate to detect precession-scale cycles throughout a record. A further difference between the two approaches is that the TimeOpt MCMC method represents a search for a combined optimisation of sedimentation rate as well as the g1-g5 and k components to fit geological and astronomical data, while our approach only searches for consistency between astronomical and geological data. As one may expect, the search for consistency allows for a larger spread in results than an optimisation of the fit.

In our opinion, the application of CTest here is not prone to bias of an individual record, because several datasets from different settings and continents provide consistent results, even though

individual datasets may be difficult to interpret alone. The considered data in this study are from rather shallow marine strata on the shelf. In such settings, one may argue that high-frequency oscillations may not be recorded and preserved as good as lower frequency components, and that longer cycles – or cycles deposited as rather thick – have higher preservation potential. It was shown in a modelling study (Fischer et al., 1991) that this may lead to a bias towards the lower frequency components especially of precession, which may result in rather long precession estimates from our study.. This seems not an issue in our case, because the contrary is found: our estimate is on the short end of precession cycle length reported for the time interval (Fig. 5), and high-frequency cycles are in average not longer than expected by theory and orbital forcing. Further, we include both obliquity- and precession components in our interpretation. Misinterpretations of either obliquity or precession components within a dataset would lead to inconsistent k determinations and no possible k reconstruction. Different interpretations of the frequency components related to precession and obliquity would result in inconsistency between individual datasets.

Our measures for Devonian Milankovitch periods are in average shorter than predicted by the empirical model of Berger & Loutre, (1994) (Fig. 5, black dashed curve), and closer to an extrapolation of the astronomical solution of Laskar et al., (2004) (Fig. 5, dotted red curve). Nevertheless, it is acknowledged that the La2004 tidal model cannot be used for extended time. Indeed, as it is based on a body tide model that is adjusted to the present tidal recession of the Moon, it would lead to a collision of the Moon and the Earth in less than 2 Ga ago, as other models including the (Walker and Zahnle, 1986) model. Interestingly, our present estimate of the precession frequency in the Devonian is in agreement with the recent physical model AstroGeo22 of (Farhat et al., 2022; Fig. 5). This model takes the possible oceanic resonances that enhance the tidal dissipative torque (Farhat et al., 2022) into account, which occur when the tidal frequency related to the spin of the Earth is close to the internal oceanic proper frequencies. In AstroGeo22, such resonances occur around 300 and 540 Ma (Farhat et al., 2022; their Fig. 4). The resulting effects are high slopes in the precession frequency variations, and a staircase shape at ~0.5-0.3 Ga (Fig. 5). Our Devonian geological data point is thus critical to validate or challenge this staircase shape of the precession variation, related to the amplitude of the oceanic tidal resonances. The cyclostratigraphic determination of the precession frequency in Zhong et al., (2020) at 445 Ma is not compatible with AstroGeo22, while the recent determination in Zhou et al., (2022) at 455 Ma is in agreement with AstroGeo22. The present determination of the precession frequency for the Devonian represents crucial evidence of the occurrence of the oceanic resonances in geological data – here at 300 and 540 Ma (Fig. 5). The available data - including ours - implies that few data points (and missing ones for times of oceanic resonances) reconstructing the Earth-Moon history, and an interpolation of these, may lead to a

simplified, and for some time intervals incorrect, planetary history because interpolation over longer times can miss resonances. Specifically, our study implies that for cyclostratigraphical and paleoclimatic studies the Farhat et al., (2022) tidal Earth-Moon evolution is capturing details of precession evolution, and their history of the Earth-moon distance should be preferred over earlier simple models. Our results further underline that the tidal dissipation was unexpectedly low during the Devonian, and the Farhat et al. (2022) model implies that this was followed by a period of large tidal dissipation during the Carboniferous, corresponding to the crossing of an oceanic tidal resonance. When comparing Farhat et al.'s (2022) model with the available geological data, the correspondence with the past rotation state provided by geological evidence is striking, also for our data point which would be considered challenging to explain in the context of the available geological data, which points to a longer precession period (Fig. 5). The Farhat et al., (2022) model is also consistent with the recent determinations of the past precession period of the Earth based on cyclostratigraphy (Huang et al., 2020; Lantink et al., 2022; Meyers and Malinverno, 2018; Sørensen et al., 2020). Consequently, we consider that the (Zhong et al., 2020) determination of the precession period at 455 Ma is challenging and worth testing. We suggest to establish multiple determinations of k for any Geological time from different (paleo)localities. Reliable and precise cyclostratigraphic determinations of precession and obliquity length in the Paleozoic Era, and specifically in the Devonian and Carboniferous Periods, are of crucial importance to fully validate – or challenge – the results of this study and the new tidat model of Farhat et al., (2022), and are expected to help better understand the amplitude effect of tidal resonances.

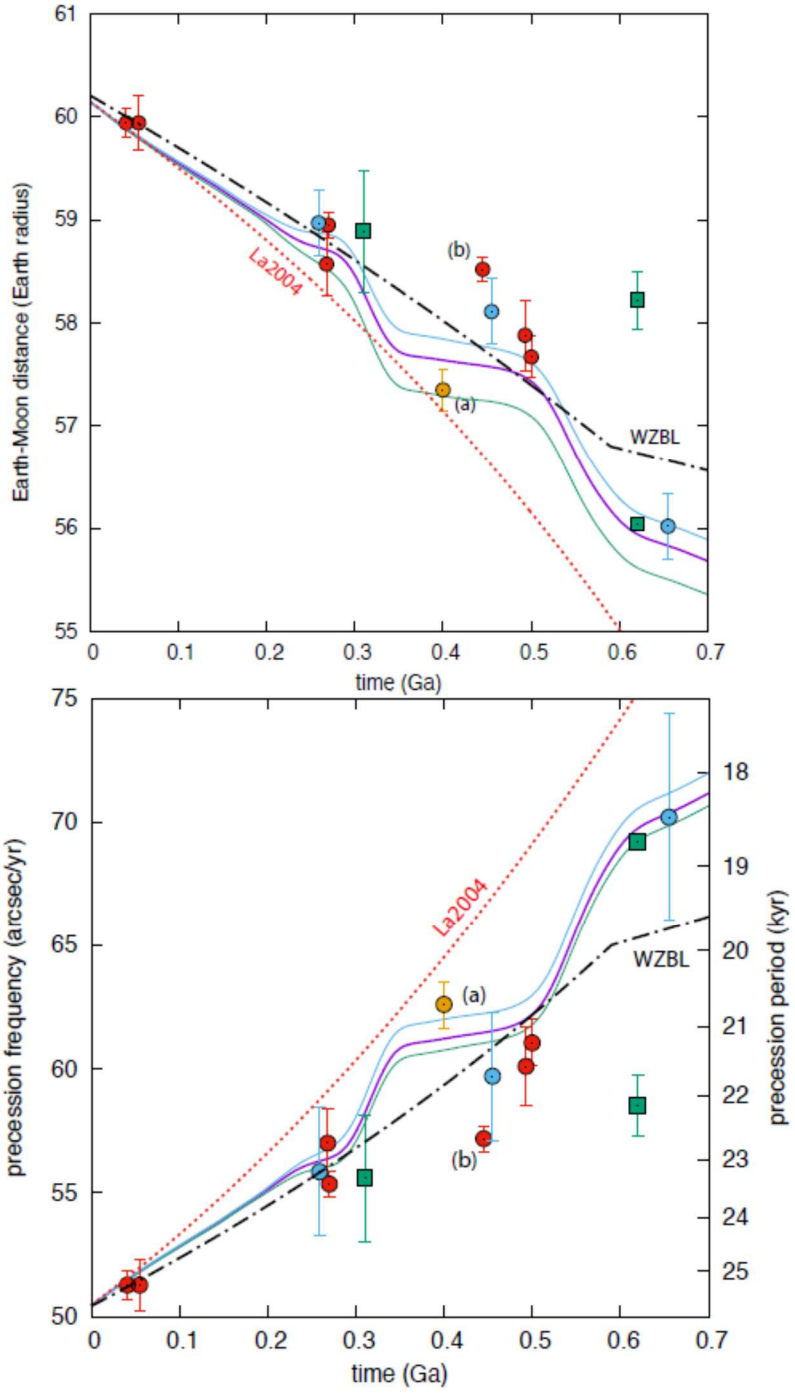

Fig. 5: Precession frequency (in arcsec/yr and as precession period; bottom) and Earth-Moon distance (in Earth radius; top) over the last 700 Ma. The yellow data point comes from this study. The solutions for Earth-Moon distance and precession of La2004 are taken both from Laskar et al, (2004). As they do not correspond to the tidal model of Farhat et al., (2022) the transfer of the precession curve of La2004 through the tidal model of Farhat et al, 2022 do not correspond to the precession curve of La2004., with uncertainty given by the blue and green side curves. The dotted red curve is extrapolated from the La2004 solution (Laskar et al., 2004; their eqs 39 and 40). The dashed black curve (WZBL) is the empirical model of (Berger and Loutre, 1994; Walker and Zahnle, 1986). The green square markers are obtained from tidal rhythmites

(Sonett and Chan, 1998; Williams, 1997, 2000). The red dots are obtained from cyclostratigraphic analysis (De Vleeschouwer et al., 2023; Fang et al., 2020; Huang et al., 2020; Meyers and Malinverno, 2018; Sørensen et al., 2020; Zhong et al., 2020). The blue dots represent cyclostratigraphic data from (Zhou et al., 2022). The red data point (b) in this figure by Zhong et al., (2020) is off the AstroGeo22 curve, but it should be noted that both the (Zhou et al., 2022; blue) and the data resulting from the present study (a) are in good agreement with AstroGeo22. The passage from precession frequency to Earth-Moon distance has been realized by interpolation using the nominal AstroGeo22 solution for all data points except for the blue points of (Zhou et al., 2022), who provide Earth-Moon distance values and associated uncertainties in their paper.

6. Acknowledgements

CZ was funded by a PSL fellowship. We acknowledge IGCP-652 project, the AstroMeso ANR-19-CE31-0002-01 project and the ERC Advanced Grant AstroGeo-885250. ACDS acknowledges the FNRS National Science Foundation grant (T.0051.19 and J.0037.21). DP was funded by SNSF Ambizione grant PZ00P2_193520. Author ACDS acknowledges the support of the CycloNet project, funded by the Research Foundation Flanders (FWO, grant nr. W000522N).

7. References Cited

Baddouh, M., Meyers, S.R., Carroll, A.R., Beard, B.L., Johnson, C.M., 2016. Lacustrine 87Sr/86Sr as a tracer to reconstruct Milankovitch forcing of the Eocene hydrologic cycle. Earth Planet. Sci. Lett. 448, 62–68. https://doi.org/10.1016/j.epsl.2016.05.007

Berger, A., Loutre, M.F., 1994. Precession, Eccentricity, Obliquity, Insolation and Paleoclimates, in: Duplessy, J.-C., Spyridakis, M.-T. (Eds.), Long-Term Climatic Variations. Springer Berlin Heidelberg, Berlin, Heidelberg, pp. 107–151.

Berger, A., Loutre, M.F., Laskar, J., 1992. Stability of the Astronomical Frequencies Over the Earth's History for Paleoclimate Studies. Science 255, 560–566. https://doi.org/10.1126/science.255.5044.560

Bond, G.C., Kominz, M.A., Beavan, J., 1991. Evidence for orbital forcing of Middle Cambrian peritidal cycles: Wah Wah range, south-central Utah. Kans. Geol. Surv. Bull. 233, 294–317.

Da Silva, A.C., De Vleeschouwer, D., Boulvain, F., Claeys, P., Fagel, N., Humblet, M., Mabille, C., Michel, J., Sardar Abadi, M., Pas, D., Dekkers, M.J., 2013. Magnetic susceptibility as a high-resolution correlation tool and as a climatic proxy in Paleozoic rocks – Merits and pitfalls: Examples from the Devonian in Belgium. Mar. Pet. Geol. 46, 173–189. https://doi.org/10.1016/j.marpetgeo.2013.06.012

Da Silva, A.C., Dekkers, M.J., De Vleeschouwer, D., Hladil, J., Chadimova, L., Slavík, L., Hilgen, F.J., 2019. Millennial-scale climate changes manifest Milankovitch combination tones and Hallstatt solar cycles in the Devonian greenhouse world: REPLY. Geology 47, e489–e490. https://doi.org/10.1130/G46732Y.1

Da Silva, A.C., Hladil, J., Chadimová, L., Slavík, L., Hilgen, F.J., Bábek, O., Dekkers, M.J., 2016. Refining the Early Devonian time scale using Milankovitch cyclicity in Lochkovian–Pragian sediments (Prague Synform, Czech Republic). Earth Planet. Sci. Lett. 455, 125–139. https://doi.org/10.1016/j.epsl.2016.09.009

Daher, H., Arbic, B.K., Williams, J.G., Ansong, J.K., Boggs, D.H., Müller, M., Schindelegger, M., Austermann, J., Cornuelle, B.D., Crawford, E.B., 2021. Long-term Earth-Moon evolution with high-level orbit and ocean tide models. J. Geophys. Res. Planets 126, e2021JE006875.

Darwin, G.H., 1879. XIII. On the precession of a viscous spheroid, and on the remote history of the Earth. Philos. Trans. R. Soc. Lond. 170, 447–538. https://doi.org/10.1098/rstl.1879.0073

De Vleeschouwer, D., Boulvain, F., Da Silva, A.-C., Pas, D., Labaye, C., Claeys, P., 2015. The astronomical calibration of the Givetian (Middle Devonian) timescale (Dinant Synclinorium, Belgium). Geol. Soc. Lond. Spec. Publ. 414, 245–256. https://doi.org/10.1144/SP414.3

De Vleeschouwer, D., Parnell, A.C., 2014. Reducing time-scale uncertainty for the Devonian by integrating astrochronology and Bayesian statistics. Geology 42, 491–494. https://doi.org/10.1130/G35618.1

De Vleeschouwer, D., Penman, D.E., D'haenens, S., Wu, F., Westerhold, T., Vahlenkamp, M., Cappelli, C., Agnini, C., Kordesch, W.E.C., King, D.J., van der Ploeg, R., Pälike, H., Turner, S.K., Wilson, P., Norris, R.D., Zachos, J.C., Bohaty, S.M., Hull, P.M., 2023. North Atlantic Drift Sediments Constrain Eocene Tidal Dissipation and the Evolution of the Earth-Moon System. Paleoceanogr. Paleoclimatology 38, e2022PA004555. https://doi.org/10.1029/2022PA004555

De Vleeschouwer, D., Vahlenkamp, M., Crucifix, M., Pälike, H., 2017. Alternating Southern and Northern Hemisphere climate response to astronomical forcing during the past 35 m.y. Geology G38663.1. https://doi.org/10.1130/G38663.1

de Winter, N.J., Goderis, S., Van Malderen, S.J.M., Sinnesael, M., Vansteenberge, S., Snoeck, C., Belza, J., Vanhaecke, F., Claeys, P., 2020. Subdaily-Scale Chemical Variability in a Torreites Sanchezi Rudist Shell: Implications for Rudist Paleobiology and the Cretaceous Day-Night Cycle. Paleoceanogr. Paleoclimatology 35, e2019PA003723. https://doi.org/10.1029/2019PA003723

436 Ebisuzaki, W., 1997. A Method to Estimate the Statistical Significance of a Correlation When the Data
437 Are Serially Correlated. J. Clim. 10, 2147–2153. https://doi.org/10.1175/1520-
438 0442(1997)010<2147:AMTETS>2.0.CO;2
439 Fang, J., Wu, H., Fang, Q., Shi, M., Zhang, S., Yang, T., Li, H., Cao, L., 2020. Cyclostratigraphy of the
440 global stratotype section and point (GSSP) of the basal Guzhangian Stage of the Cambrian
441 Period. Palaeogeogr. Palaeoclimatol. Palaeoecol. 540, 109530.
442 https://doi.org/10.1016/j.palaeo.2019.109530
443 Fang, Q., Wu, H., Hinnov, L.A., Wang, X., Yang, T., Li, H., Zhang, S., 2016. A record of astronomically
444 forced climate change in a late Ordovician (Sandbian) deep marine sequence, Ordos Basin,
445 North China. Sediment. Geol. 341, 163–174. https://doi.org/10.1016/j.sedgeo.2016.06.002
446 Farhat, M., Auclair-Desrotour, P., Boué, G., Laskar, J., 2022. The resonant tidal evolution of the Earth-
447 Moon distance. Astron. Astrophys. 665, L1. https://doi.org/10.1051/0004-6361/202243445
448 Fischer, A.G., Herbert, T.D., Napoleone, G., Silva, I.P., Ripepe, M., 1991. Albian Pelagic Rhythms
449 (Piobbico Core). J. Sediment. Res. 61.
450 Gerstenkorn, H., 1967. On the controversy over the effect of tidal friction upon the history of the
451 earth-moon system. Icarus 7, 160–167. https://doi.org/10.1016/0019-1035(67)90060-7
452 Green, J.A.M., Huber, M., Waltham, D., Buzan, J., Wells, M., 2017. Explicitly modelled deep-time tidal
453 dissipation and its implication for Lunar history. Earth Planet. Sci. Lett. 461, 46–53.
454 https://doi.org/10.1016/j.epsl.2016.12.038
455 Heubeck, C., Biasing, S., Grund, M., Drabon, N., Homann, M., Nabhan, S., 2016. Geological constraints
456 on Archean (3.22 Ga) coastal-zone processes from the Dycedale Syncline, Barberton
457 Greenstone Belt. South Afr. J. Geol. 119, 495–518. https://doi.org/10.2113/gssajg.119.3.495
458 Hilgen, F.J., Hinnov, L.A., Aziz, H.A., Abels, H.A., Batenburg, S., Bosmans, J.H.C., Boer, B. de, Hüsing,
459 S.K., Kuiper, K.F., Lourens, L.J., Rivera, T., Tuenter, E., Wal, R.S.W.V. de, Wotzlaw, J.-F., Zeeden,
460 C., 2015. Stratigraphic continuity and fragmentary sedimentation: the success of
461 cyclostratigraphy as part of integrated stratigraphy. Geol. Soc. Lond. Spec. Publ. 404, 157–197.
462 https://doi.org/10.1144/SP404.12
463 Hinnov, L.A., 2013. Cyclostratigraphy and its revolutionizing applications in the earth and planetary
464 sciences. Geol. Soc. Am. Bull. 125, 1703–1734. https://doi.org/10.1130/B30934.1
465 Hinnov, L.A., Hilgen, F.J., 2012. Chapter 4 - Cyclostratigraphy and Astrochronology, in: Gradstein, F.M.,
466 Ogg, J.G., Schmitz, M.D., Ogg, G.M. (Eds.), The Geologic Time Scale. Elsevier, Boston, pp. 63–
467 83.
468 Huang, H., Gao, Y., Jones, M.M., Tao, H., Carroll, A.R., Ibarra, D.E., Wu, H., Wang, C., 2020.
469 Astronomical forcing of Middle Permian terrestrial climate recorded in a large paleolake in
470 northwestern China. Palaeogeogr. Palaeoclimatol. Palaeoecol. 550, 109735.
471 https://doi.org/10.1016/j.palaeo.2020.109735
472 Huybers, P., Aharonson, O., 2010. Orbital tuning, eccentricity, and the frequency modulation of
473 climatic precession. Paleoceanography 25. https://doi.org/10.1029/2010PA001952
474 Lantink, M.L., Davies, J.H.F.L., Ovtcharova, M., Hilgen, F.J., 2022. Milankovitch cycles in banded iron
475 formations constrain the Earth–Moon system 2.46 billion years ago. Proc. Natl. Acad.
476 Sci. 119, e2117146119. https://doi.org/10.1073/pnas.2117146119
477 Laskar, J., Fienga, A., Gastineau, M., Manche, H., 2011a. La2010: a new orbital solution for the long-
478 term motion of the Earth. Astron. Astrophys. 532, A89. https://doi.org/10.1051/0004-
479 6361/201116836
480 Laskar, J., Gastineau, M., Delisle, J.-B., Farrés, A., Fienga, A., 2011b. Strong chaos induced by close
481 encounters with Ceres and Vesta. Astron. Astrophys. 532, L4. https://doi.org/10.1051/0004-
482 6361/201117504
483 Laskar, J., Robutel, P., Joutel, F., Gastineau, M., Correia, A.C.M., Levrard, B., 2004. A long-term
484 numerical solution for the insolation quantities of the Earth. Astron. Astrophys. 428, 261–285.
485 https://doi.org/10.1051/0004-6361:20041335

Lourens, L.J., Wehausen, R., Brumsack, H.J., 2001. Geological constraints on tidal dissipation and dynamical ellipticity of the Earth over the past three million years. Nature 409, 1029–1033. https://doi.org/10.1038/35059062

Mabille, C., Boulvain, F., 2008. Les Monts de Baileux section: detailed sedimentology and magnetic susceptibility of Hanonet, Trois-Fontaines and Terres d'Haurs formations (Eifelian-Givetian boundary and Lower Givetian, SW Belgium). Geol. Belg. 11.

Maurice, M., Tosi, N., Schwinger, S., Breuer, D., Kleine, T., 2020. A long-lived magma ocean on a young Moon. Sci. Adv. 6, eaba8949. https://doi.org/10.1126/sciadv.aba8949

Meyers, S.R., 2015. The evaluation of eccentricity-related amplitude modulation and bundling in paleoclimate data: An inverse approach for astrochronologic testing and time scale optimization. Paleoceanography 30, 1625–1640. https://doi.org/10.1002/2015PA002850

Meyers, S.R., 2014. astrochron: An R Package for Astrochronology Version 0.9.

Meyers, S.R., Malinverno, A., 2018. Proterozoic Milankovitch cycles and the history of the solar system. Proc. Natl. Acad. Sci. 201717689. https://doi.org/10.1073/pnas.1717689115

Pas, D., Da Silva, A.-C., Devleeschouwer, X., De Vleeschouwer, D., Cornet, P., Labaye, C., Boulvain, F., 2017. Insights into a million-year-scale Rhenohercynian carbonate platform evolution through a multi-disciplinary approach: example of a Givetian carbonate record from BelgiumD. PAS AND OTHERSGivetian carbonate record from Belgium. Geol. Mag. 154, 707–739. https://doi.org/10.1017/S00167568

Pas, D., Hinnov, L., Day, J.E. (Jed), Kodama, K., Sinnesael, M., Liu, W., 2018. Cyclostratigraphic calibration of the Famennian stage (Late Devonian, Illinois Basin, USA). Earth Planet. Sci. Lett. 488, 102–114. https://doi.org/10.1016/j.epsl.2018.02.010

Ruddiman, W.F., 2001. Earth's climate: past and future. Freeman.

Shackleton, N.J., Hagelberg, T.K., Crowhurst, S.J., 1995. Evaluating the success of astronomical tuning: Pitfalls of using coherence as a criterion for assessing pre-Pleistocene timescales. Paleoceanography 10, 693–697. https://doi.org/10.1029/95PA01454

Sonett, C.P., Chan, M.A., 1998. Neoproterozoic Earth-Moon dynamics: Rework of the 900 Ma Big Cottonwood Canyon tidal laminae. Geophys. Res. Lett. 25, 539–542. https://doi.org/10.1029/98GL00048

Sørensen, A.L., Nielsen, A.T., Thibault, N., Zhao, Z., Schovsbo, N.H., Dahl, T.W., 2020. Astronomically forced climate change in the late Cambrian. Earth Planet. Sci. Lett. 548, 116475. https://doi.org/10.1016/j.epsl.2020.116475

Tyler, R.H., 2021. On the Tidal History and Future of the Earth–Moon Orbital System. Planet. Sci. J. 2, 70. https://doi.org/10.3847/psj/abe53f

Walker, J.C.G., Zahnle, K.J., 1986. Lunar nodal tide and distance to the Moon during the Precambrian. Nature 320, 600–602. https://doi.org/10.1038/320600a0

Waltham, D., 2015. Milankovitch Period Uncertainties and Their Impact On Cyclostratigraphy. J. Sediment. Res. 85, 990–998. https://doi.org/10.2110/jsr.2015.66

Webb, D.J., 1980. Tides and tidal friction in a hemispherical ocean centred at the equator. Geophys. J. Int. 61, 573–600. https://doi.org/10.1111/j.1365-246X.1980.tb04833.x

Williams, G.E., 2000. Geological constraints on the Precambrian history of Earth's rotation and the Moon's orbit. Rev. Geophys. 38, 37–59. https://doi.org/10.1029/1999RG900016

Williams, G.E., 1997. Precambrian length of day and the validity of tidal rhythmite paleotidal values. Geophys. Res. Lett. 24, 421–424. https://doi.org/10.1029/97GL00234

Williams, G.E., 1991. Milankovitch-band cyclicity in bedded halite deposits contemporaneous with Late Ordovician-Early Silurian glaciation, Canning Basin, Western Australia. Earth Planet. Sci. Lett. 103, 143–155. https://doi.org/10.1016/0012-821X(91)90156-C

Williams, G.E., 1989. Tidal Rhythmites: Geochronometers for the Ancient Earth-Moon System. Episodes 12, 162–171.

Williams, J.G., Boggs, D.H., 2016. Secular tidal changes in lunar orbit and Earth rotation. Celest. Mech. Dyn. Astron. 126, 89–129. https://doi.org/10.1007/s10569-016-9702-3

Wu, H., Fang, Q., Wang, X., Hinnov, L.A., Qi, Y., Shen, S., Yang, T., Li, H., Chen, J., Zhang, S., 2018. An ~34 m.y. astronomical time scale for the uppermost Mississippian through Pennsylvanian of the Carboniferous System of the Paleo-Tethyan realm. Geology. https://doi.org/10.1130/G45461.1

Wu, H., Zhang, S., Hinnov, L.A., Jiang, G., Feng, Q., Li, H., Yang, T., 2013. Time-calibrated Milankovitch cycles for the late Permian. Nat. Commun. 4, 2452. https://doi.org/10.1038/ncomms3452

Zachos, J.C., 2004. Proc. ODP, Init. Repts., 208: Coll. Stn. TX Ocean Drill. Program 208. https://doi.org/10.2973/odp.proc.ir.208.2004

Zeeden, C., Hilgen, F., Westerhold, T., Lourens, L., Röhl, U., Bickert, T., 2013. Revised Miocene splice, astronomical tuning and calcareous plankton biochronology of ODP Site 926 between 5 and 14.4 Ma. Palaeogeogr. Palaeoclimatol. Palaeoecol. 369, 430–451. https://doi.org/10.1016/j.palaeo.2012.11.009

Zeeden, C., Hilgen, F.J., Hüsing, S.K., Lourens, L.L., 2014. The Miocene astronomical time scale 9–12 Ma: New constraints on tidal dissipation and their implications for paleoclimatic investigations. Paleoceanography 29, 2014PA002615. https://doi.org/10.1002/2014PA002615

Zeeden, C., Meyers, S.R., Hilgen, F.J., Lourens, L.J., Laskar, J., 2019. Time scale evaluation and the quantification of obliquity forcing. Quat. Sci. Rev. 209, 100–113. https://doi.org/10.1016/j.quascirev.2019.01.018

Zeeden, C., Meyers, S.R., Lourens, L.J., Hilgen, F.J., 2015. Testing astronomically tuned age models. Paleoceanography 30, 2014PA002762. https://doi.org/10.1002/2014PA002762

Zhang, S., Wang, X., Hammarlund, E.U., Wang, H., Costa, M.M., Bjerrum, C.J., Connelly, J.N., Zhang, B., Bian, L., Canfield, D.E., 2015. Orbital forcing of climate 1.4 billion years ago. Proc. Natl. Acad. Sci. 112, E1406–E1413. https://doi.org/10.1073/pnas.1502239112

Zhong, Y., Wu, H., Fan, J., Fang, Q., Shi, M., Zhang, S., Yang, T., Li, H., Cao, L., 2020. Late Ordovician obliquity-forced glacio-eustasy recorded in the Yangtze Block, South China. Palaeogeogr. Palaeoclimatol. Palaeoecol. 540, 109520. https://doi.org/10.1016/j.palaeo.2019.109520

Zhou, M., Wu, H., Hinnov, L.A., Fang, Q., Zhang, S., Yang, T., Shi, M., 2022. Empirical Reconstruction of Earth-Moon and Solar System Dynamical Parameters for the Past 2.5 Billion Years From Cyclostratigraphy. Geophys. Res. Lett. 49, e2022GL098304. https://doi.org/10.1029/2022GL098304